Numerical analysis of effective hybrid sandwiched reinforcement for cohesive soils

Yamazaki, S., Yasuhara, K., Komine, H. & Murakami, S.
Department of Urban and Civil Engineering, Ibaraki University, Hitachi, Ibaraki, Japan

Mohri, H. & Hori, T.
Joint Researcher of Soil Mechanics Labs, National Institute for Rural Engineering, Tsukuba, Ibaraki, Japan

Keywords: geosynthetics , sandwiched method , numerical analysis

ABSTRACT: We developed a new construction technique called Hybrid Sandwiched Reinforcement (HBS) method, by which thin sand layers are placed above and beneath a geosynthetic fabric to increase the mechanical potential of cohesive soil embankments and foundations. This reinforcement method improves reinforcement and maintains hydraulic conductivity. Successive to the authors' previous works, this paper describes numerical analysis of embankment with and without reinforcement and a sand layer.
Results from numerical analyses are interpreted with emphasis on improved toughness of HBS-reinforced embankments. Results clarified that HBS not only controls embankment deformation, it improves toughness using placement of geosynthetics in an embankment comprising cohesive soils such as Kanto loam of volcanic-ash origin. Regarding improved toughness of HBS earth structures, the numerical analysis results show that the sandwich structure improves the cohesive soil embankments' bearing capacity and stiffness. Placement of thin sand layers above and below non-woven geosynthetics and their high potential for drainage make non-woven geosynthetics more suitable for sandwiched earth structures consisting of cohesive soils, particularly cohesive soils of volcanic origin. Results are superior to those of geonets or geogrids, which are widely used for sandy soil reinforcement.

1 INTRODUCTION

Great demand has arisen for effective utilization of high-water-content cohesive soil because of a lack of good soil and difficulty securing construction sites. For those reasons, we developed a construction technique called Hybrid Sandwiched Reinforcement (HBS) method (see Figure 1), by which thin sand layers are placed on and beneath geosynthetic fabric (GS) to increase cohesive soil embankments' and foundations' mechanical potential. The HBS method is used together with a sand layer for protection of non-woven clogging and for a new function: toughness improvement. This reinforcement method is advantageous for reinforcement improvement and retention of hydraulic conductivity. Both are greater than in cases of reinforcement without the sand layer. Results of earlier studies (Sakakibara et al., 2005;Yasuhara et al., 2006; Yamazaki et al., 2007) show that hybrid sandwiched reinforcement (HBS), by which geosynthetics are placed in cohesive soil embankments with thin sandwiched sand layers, has provided many benefits. Successive to the authors' previous works, we performed numerical analyses of embankments with and without reinforcement, and with and without the sand layer.

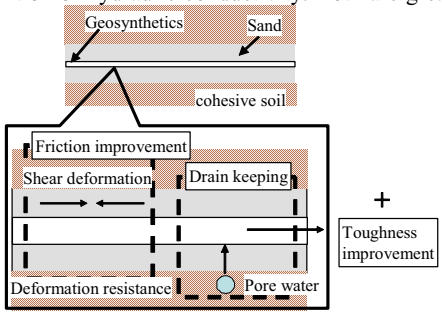

Figure 1. Outline of HBS method

2 OUTLINE OF NUMERICAL ANALYSIS

2.1 *Outline*

We performed numerical analysis using the same conditions as those of the model test (Yamazaki et al., 2007) using a numerical analysis program (GEOCUP; Kohgo, 1995) developed at Tokyo University of Agriculture and Technology. The model uses FEM analysis with an elasto-plastic model. We examined non-reinforced embankment, reinforced embankment, HBS method embankment, GS, sand layer effects, and embankment behavior. We devoted particular attention to effects of the (a) HBS method, (b) single-layer GS position, (c) sand thickness, (d) the GS type, and (e) a reinforced layer.

2.2 *Analysis model*

The analysis model is 40.5 cm high with a slope gradient of 1:0.5. Volcanic Kanto loam was used as the embankment material, with a Toyoura sand layer. Figure 2 shows a numerical analysis outline.

The yield function of the soil material adopted Mohr–Coulomb type and used an eight node quadrangle element. In addition, GS presumed elastic body, modulus of elasticity calculated by tensile test. We used GS of two types: non-woven GS had 5.8 kN/m tensile strength (strain 110%) and permeability; Geonet had 3.6 kN/m tensile strength (strain 10.6%). Table 1 shows numerical analysis cases.

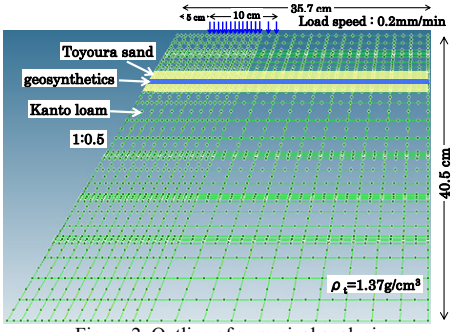

Figure 2. Outline of numerical analysis

Table 1. Numerical analysis case

Case	Reinforced method	Geosynthetics	Sand thickness	Layer	Single Layer depth
1	Non-reinforcement	—	—	—	—
2	Non-woven + sand	Non-woven	1 cm	1 (top)	2 cm
3	Non-woven + sand	Non-woven	1 cm	1 (top)	4.5 cm
4	Non-woven + sand	Non-woven	1 cm	1 (top)	7 cm
5	Sand	—	1 cm	1 (top)	4.5 cm
6	Non-woven	Non-woven	—	1 (top)	4.5 cm
7	Sand	—	3 cm	1 (top)	4.5 cm
8	Non-woven + sand	Non-woven	3 cm	1 (top)	4.5 cm
9	Geonets	Geonets	—	1 (top)	4.5 cm
10	Geonets + sand	Geonets	3 cm	1 (top)	4.5 cm
11	Non-woven + sand	Non-woven	1 cm	2	4.5 cm
12	Non-woven + sand	Non-woven	1 cm	3	4.5 cm

2.3 *Analysis parameters*

Material parameters were determined from tri-axial compression and permeability tests. Table 2 shows those for Kanto loam used in numerical analysis.

Table 2. Kanto loam parameters used for numerical analysis

Initial shear modulus: G_0=500	Intercept of normal consolidation curve: Γ =4.303
Shear modulus: γ_J=50.27	Consolidation yield stress: p_c=163 kN/m^2
Angle of Mohr-Coulomb's failure criterion: ϕ '=27.9 °	Mean effective stress of Initial void ratio: p_0=81.35 kN/m^2
Compression index: λ =0.686	Coefficient of permeability: k=6.29×10^{-8} cm/s
Expansion index: κ =0.013	
Modulus of elasticity	Non-woven : 6.5 kN/m^2 Geonet : 70 kN/m^2

3 RESULTS OF NUMERICAL ANALYSIS

3.1 *Effect of HBS method*

The HBS method effects were confirmed in cases 1, 6, 7, and 8, as shown in Figure 3. Figure 4 shows settlement of the embankment with loading pressure in cases 1, 6, 7, and 8. Figures 5–11 show numerical analysis results with 240 kN/m2 loading pressure. Additionally, we calculated the slope displacement twice to show the difference of displacement.

Figures 4 and 5 show that the top of the slope exhibited large deformation in case 1 (non-reinforcement); the maximum displacement was about 2.5 cm. Moreover, the maximum displacement was about 1.2 cm in case 8 (non-woven + sand). Results confirmed that conditions in case 8 improved rigidity and deformation using HBS method. Sliding occurred using GS material in case 6 (non-woven).

Next, Figures 6 and 7 show that the maximum shear strain developed from the crest to depth 20 cm in case 1 (non-reinforcement). However, no strain occurred under GS in case 8 (HBS). We considered that GS checked stress transmission to the area be-

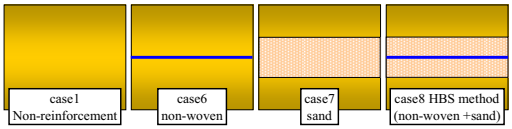

Figure 3. Test case Effect of HBS method

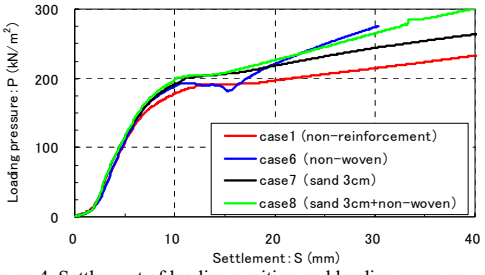

Figure 4. Settlement of loading position and loading pressure (effect of HBS method)

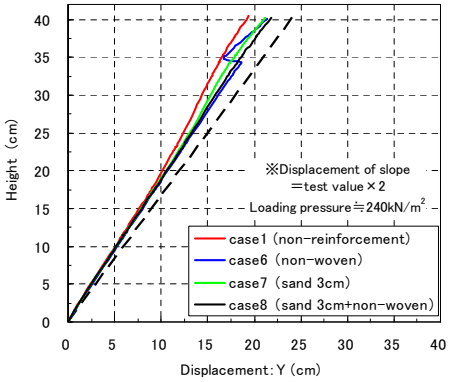

Figure 5. Slope displacement (effect of HBS method)

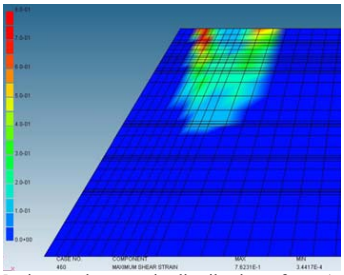

Figure 6. Maximum shear strain distribution of case1 (non-reinforcement) with loading pressure of 240 kN/m^2

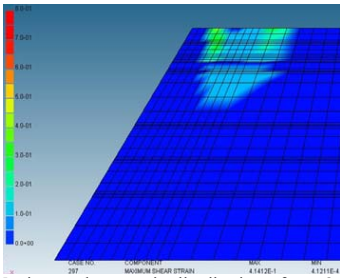

Figure 7. Maximum shear strain distribution of case8 (sand 3cm + non-woven) with loading pressure of 240 kN/m^2

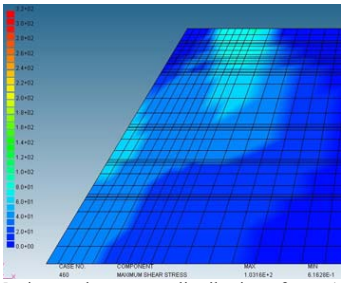

Figure 8. Maximum shear stress distribution of case1 (non-reinforcement) with loading pressure of 240 kN/m^2

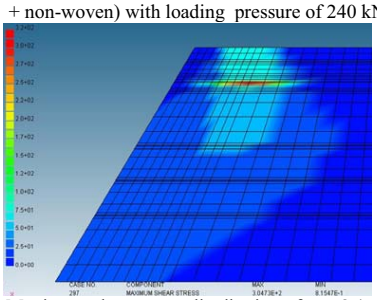

Figure 9. Maximum shear stress distribution of case8 (sand 3cm + non-woven) with loading pressure of 240 kN/m^2

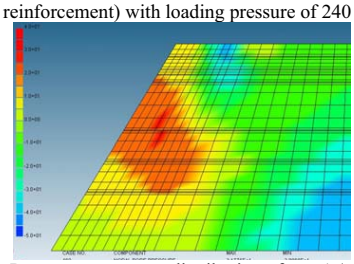

Figure 10. Pore water pressure distribution of case1 (non-reinforcement) with loading pressure of 240 kN/m^2

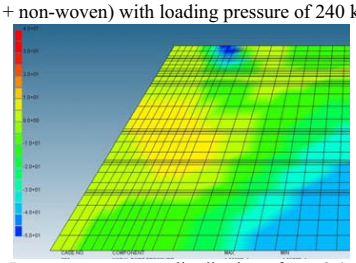

Figure 11. Pore water pressure distribution of case8 (sand 3cm + non-woven) with loading pressure of 240 kN/m^2

low the embankment and that the friction force between GS and sand was present.

From Figures 8 and 9, maximum shear stress of case8 (HBS) developed compare with case1 (non-reinforcement). The tensile stress of GS works, causing a reinforcement effect in case 8 (HBS). Next, Figures 10 and 11 show a large pore water pres-sure on the embankment hillside in case 1 (non-reinforcement). However, the pore water pressure of case 8 (HBS) shows a small range of incidence, showing a drainage function influenced by the non-woven fabric and sand.

Here in before, the stress transmission function by friction force was demonstrated between the sand and GS, showing a reinforcement effect. The slope displacement was restrained, which shows the importance of improving the boundary between GS and Kanto loam. The HBS method is superior to reinforced earth.

3.2 *Influence of single- layer GS position*

We confirmed the influence of single-layer GS position on the HBS effect in cases 2, 3, and 4 in Figure 12. Figure 13 shows settlement of the embankment with loading pressure in cases 2, 3, and 4. Figures 14–17 show numerical analysis results with loading pressure of 240 kN/m^2. Additionally, we calculated the slope displacement twice to show the difference

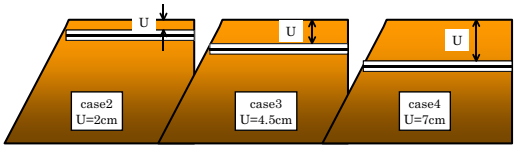

Figure 12. Test case influence of one layer's GS position

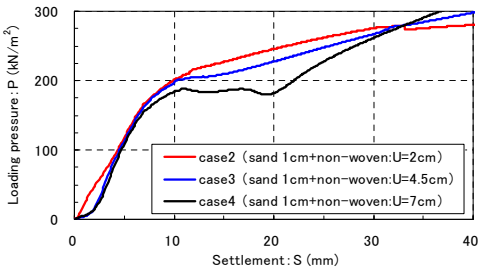

Figure 13. Settlement of loading position and loading pressure (influence of single-layer GS position)

of displacement.
Figure 13 also shows case 2 (U=2 cm) as the most rigid, although settlement is 20 cm. However, case 4 (U=7 cm) has the most rigid downward settlement of 30 cm. The HBS effect of case 4 (U=7 cm) was displayed accompanying the increased loading. However, the embankment underwent slope failure above the reinforcement layer position in case 4 (U=7 cm), as shown in Figure 14. Figures 15 and 16 confirmed a slide on the GS. The GS effect occurred slowly because of the GS position depth. The slide occurred above the GS.
Next, Figure 17 shows the maximum tensile stress of GS and settlement of the loading position. From Fig. 3.15, settlement of case 2 (U=2 cm) is small and tensile stress was displayed in the same loading pressure. Nevertheless, the loading advance, tensile stress of case 3 (U=4.5 cm) and case 4 (U=7 cm) increased gradually.
A slide occurred in case 4 (U=7 cm); GS was laid in a deep position from the crest before the reinforcement effect was exercised. In contrast, the reinforcement effect and settlement control effect were exercised early in case 2 (U=2 cm). However, it is not efficient because of the low tensile stress. Therefore, case 3 (U=4.5 cm) is an appropriate position U (a deep position from crest)/B (loading width) = 0.45. In other words, GS must be arranged effectually for the loading dispersion effect to contribute stability.

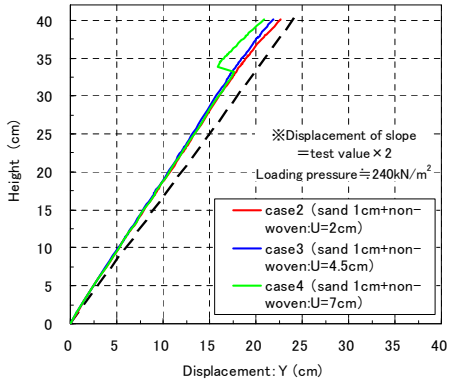

Figure 14. Slope displacement (influence of single-layer GS position)

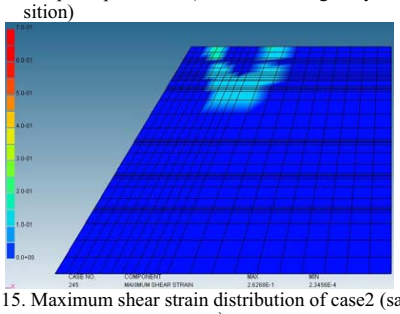
Figure 15. Maximum shear strain distribution of case2 (sand 1cm+ non-woven U=2cm) with loading pressure of 240 kN/m^2

3.3 *Influence of sand thickness*

We confirmed the influence of sand thickness on stability by case 3, 5, 7 and 8 in Figure 18. Figure 19 shows settlement of the embankment with loading pressure in cases 3, 5, 7, and 8. Figure 20 shows numerical analysis results that occur with loading pressure of 240 kN/m^2. Additionally, we calculated the slope displacement twice to show differences of displacement.
Cases 3 and 8 use HBS method (non-woven + sand); cases 5 and 7 use only sand. The sand thick-nesses in cases 3 and 5 are 1 cm; those of cases 8 and 7 are 3 cm. Comparison of the former and the latter shows that the increases of the settlement rate on loading pressure were equivalent. Furthermore, case 5 and case 7 show the same slope displacement as those in case 3 and case 8. Furthermore, shear strain distribution and shear strain distribution show similar tendencies between case 5 and case 7, and between case 3 and case 8.
Therefore, sand thickness led to no differences. Consequently, sand thickness must increase the friction force between GS and sand function of the buffer material. The friction force reinforcement effect is unrelated to the sand thickness. Model tests show the same result.

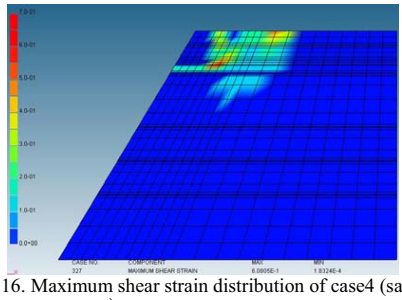
Figure 16. Maximum shear strain distribution of case4 (sand 1cm +non-woven U=7cm) with loading pressure of 240 kN/m^2

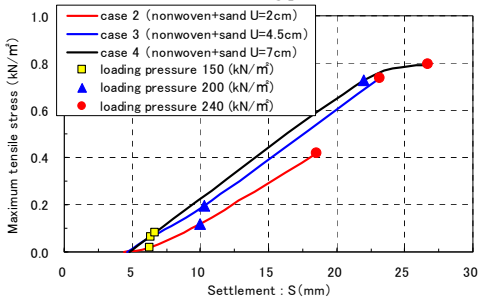

Figure 17. Maximum tensile stress of GS and settlement of the loading position (influence of single-layer GS position)

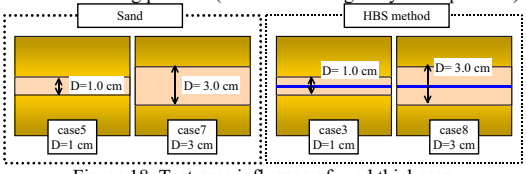

Figure 18. Test case influence of sand thickness

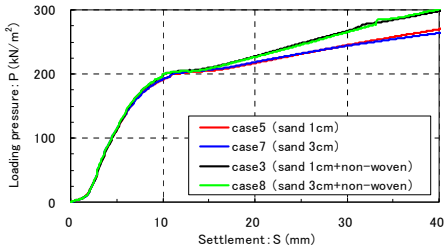

Figure 19. Settlement of the loading position and loading pressure (influence of sand thickness)

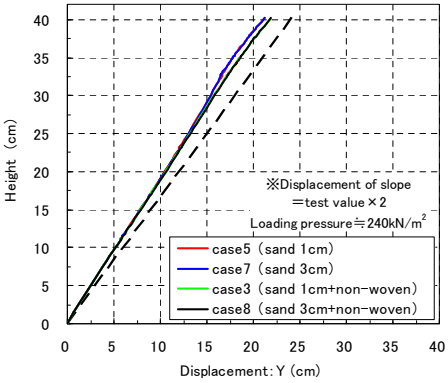

Figure 20. Slope displacement (influence of sand thickness)

3.4 *Influence of kind of GS*

We confirmed that the GS type influences embankment stability by case 6, 8, 9, and 10 shown Figure 21.

Figure 22 depicts settlement of the embankment with loading pressure in cases 6, 8, 9, and 10. Figures 23–28 show numerical analysis results that occur with loading pressure of 240 kN/m^2. Additionally, we calculated the slope displacement twice to show the difference of displacement.

Figures 22 and 23 show no clear difference in results of non-woven (cases 6 and 8) and Geonet (cases 9 and 10) for rigidity. Sliding occurred above the GS in case 6 (non-woven). How-ever, for loading pressure increasing after the slide, case 6 (non-woven) has high durability. Case 8 (non-woven and sand) and case 10 (geonet and sand) show no clear difference.

Next, as shown in Figures 24 and 25, large shear strain occurred above the GS. This appeared also in case 9 (geonet). Case 8 (non-woven + sand) shows no large shear strain, with case 10 (geonet + sand) showing the same tendency. Figure 26 shows the tensile stress of GS and the distance from the slope. A comparison of case 6 (non-woven) and case 9 (geonet) shows that case 6 (non-woven) has large tensile stress. Comparison of case 8 (non-woven + sand) and case 10 (geonet + sand) shows that case 10 (geonet + sand) has large tensile stress. Therefore, the non-woven system is advantageous in cases using single-layer GS because non-woven cases show a drainage effect. However, for sand use, geonet is advantageous because of the friction force between GS and sand.

Figures 27 and 28 present a comparison of case 6 (non-woven) and case 9 (geonet), where case 6 (non-woven) shows occurrence of water pressure. They show the drainage function of the non-woven material. Case 8 (non-woven + sand) and case 10 (geonet + sand) show occurrence of water pressure for non-woven materials and the sand drain effect.

We confirmed the effectiveness in single laid GS, the non-woven material: its coefficient of permeability is larger than that of geonet. However, for GS with sand (HBS method) the friction force was more effective using geonet than with non-woven material. However, each geonet and non-woven showed larger tensile stress and control slope displacement than single GS.

Results confirmed the friction force of soil and GS. Boundary plane improvement is important.

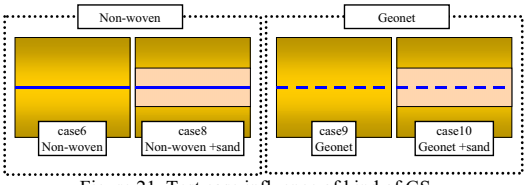

Figure 21. Test case influence of kind of GS

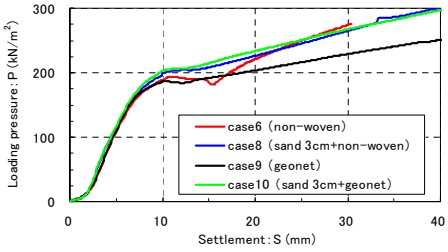

Figure 22. Settlement of loading position and loading pressure (influence of kind of GS)

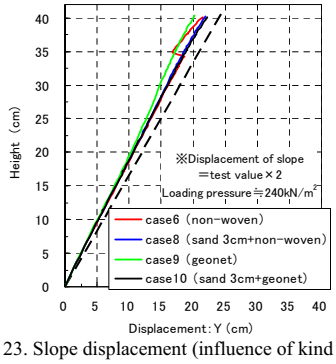

Figure 23. Slope displacement (influence of kind of GS)

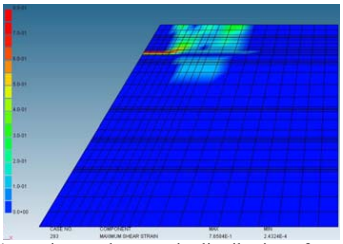

Figure 24. maximum shear strain distribution of case6 (non-woven) with loading pressure of 240 kN/m^2

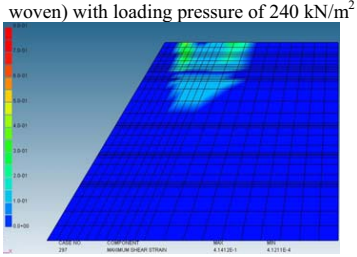

Figure 25. Maximum shear strain distribution of case8 (sand 3cm + non-woven) with loading pressure of 240 kN/m^2

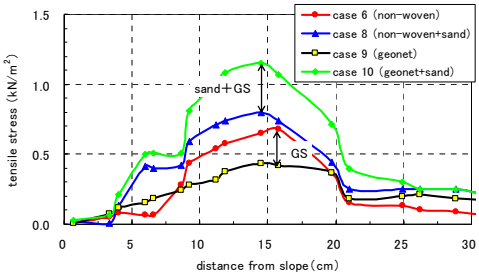

Figure 26. tensile stress and distance from slope in loading pressure 240 kN/m^2

4 CONCLUSION

Numerical analysis using finite element method was conducted to assess the advantageous features of HBS reinforcement.

i) Bearing capacity and stiffness of embankments made with cohesive soils are improved by the sandwiched structure, in which thin sand layers are placed above and below unwoven GS.

ii)A GS reinforced sandwiched embankment provides high resilience, leading to stable earth structures, suggesting that sandwiched structures are expected to resist earth-quake damage.

iii) The sand layer thickness used for the sandwiched structure is unrelated to improvement of the embankment's bearing capacity, stiffness, and resilience.

iv)The tensile strength of non-woven GS laid at the shallow depth of an embankment is exhibited from the early stage of load application, but it is not so great. However, reinforcement effects of GS placed at a deep location of an embankment are exerted only when a large slip failure circle occurs.

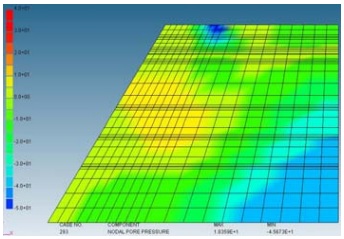

Figure 27. Pore water pressure distribution of case6 (non-woven) with loading pressure of 240 kN/m^2

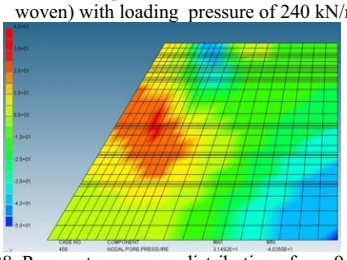

Figure 28. Pore water pressure distribution of case9 (geonet) with loading pressure of 240 kN/m^2

v) Because of their high potential for drainage, unwoven GS are more suitable for sandwiched earth structures consisting of cohesive soils, particularly cohesive soils of volcanic origin, than are geonet or geogrid, which are popularly used for sandy soil reinforcement.

REFERENCES

Kohgo, Y. 1995. On mechanical properties of unsaturated soils and stability analyses of soil structures, *Proc. of Bulletin of the national for rural engineering*, Vol. 34, pp. 42-159. (in Japanese).

Sakakibara, T., Yasuhara, K., Murakami, S. & H.Komine. 2005. Toughness improvement using hybrid-sandwich earth structures with geosynthetics, *Proc. of Geosynthetics Engineering Journal*, Vol. 20, pp. 81-88. (in Japanese)

Yamazaki, S. & Yasuhara, K. 2006. Influencing factors on toughness improvement of hybrid sandwich reinforced embankment, *Proc. of Geosynthetics Engineering Journal*, Vol. 21, pp. 81-88. (in Japanese)

Yamazaki, S., Yasuhara, K., Murakami, S. & Komine, H. 2007. Toughness improvement of hybrid sandwiched foundations and embankment reinforced with geosynthetics, *Proc. of the 5th International Symposium on Earth Rein-forcement* (IS Kyushu'07), pp. 673-680.

Yamazaki, S., Yasuhara, K. & Sato, T. 2006. Effect of improvement toughness by hybrid-sandwich method, *Proc. of Japanese Society of Civil Engineers 61th*, pp. 79-80. (in Japanese).

Yasuhara, K., Ghosh, C., Sakakibara, T., Murakami, S. & Komine, H. 2004. Advantage aspects of hybrid-sandwich type reinforced earth, *Proc. of Geosynthetics Engineering Journal*, Vol. 19, pp. 139-146. (in Japanese)

Yasuhara, K., Murakami, S., Komine, H. & Sakakibara, T. 2006. Hybrid-sandwiched foundations reinforced with geosynthetics, *Proc. of Geosynthetics 8th ICG*, pp. 1005-1010.